Synthesis and Characterization of Photo-Cross-Linked Hydrogels Based on Biodegradable Polyphosphoesters and Poly(ethylene glycol) Copolymers

Jin-Zhi Du,[†] Tian-Meng Sun,[‡] Song-Qing Weng,[†] Xue-Si Chen,[§] and Jun Wang*[,†,‡]

Department of Polymer Science and Engineering and Hefei National Laboratory for Physical Sciences at Microscale and School of Life Sciences, University of Science and Technology of China, Hefei, Anhui 230026, P.R. China, and State Key Laboratory of Polymer Physics and Chemistry, Changchun Institute of Applied Chemistry, Chinese Academy of Sciences, Changchun 130022, P. R. China

Received April 30, 2007; Revised Manuscript Received August 2, 2007

Novel biodegradable hydrogels by photo-cross-linking macromers based on polyphosphoesters and poly(ethylene glycol) (PEG) are reported. Photo-cross-linkable macromers were synthesized by ring-opening polymerization of the cyclic phosphoester monomer 2-(2-oxo-1,3,2-dioxaphospholoyloxy) ethyl methacrylate (OPEMA) using PEG as the initiator and stannous octoate as the catalyst. The macromers were characterized by ^{1}H NMR, Fourier transform infrared spectroscopy, and gel permeation chromatography measurements. The content of polyphosphoester in the macromer was controlled by varying the feed ratio of OPEMA to PEG. Hydrogels were fabricated by exposing aqueous solutions of macromers with 0.05% (w/w) photoinitiator to UV light irradiation, and their swelling kinetics as well as degradation behaviors were evaluated. The results demonstrated that cross-linking density and pH values strongly affected the degradation rates. The macromers was compatible to osteoblast cells, not exhibiting significant cytotoxicity up to 0.5 mg/mL. "Live/dead" cell staining assay also demonstrated that a large majority of the osteoblast cells remained viable after encapsulation into the hydrogel constructs, showing their potential as tissue engineering scaffolds.

1. Introduction

Hydrogels have attracted extensive attention in biomedical fields as drug and gene delivery matrixes and tissue engineering scaffolds because of their biocompatibility and resemblance to biological tissues.[1−7] Many fabrication methods have been utilized for hydrogel construction,[8−10] among which photo-cross-linking is attractive since it allows hydrogels to be generated in situ from a low-viscosity solution of monomers or macromers. It offers fast curing at physiological temperatures, therefore the hydrogel can be placed into critical defects in a minimally invasive manner to promote tissue regeneration.[11,12] For example, it has been successfully applied for cartilage tissue engineering in supporting chondrocytes survival and cartilage matrix synthesis.[13−16]

In addition to possessing the requirements to promote the adhesion, proliferation, and function of cells encapsulated in the hydrogel constructs, hydrogels for tissue regeneration are generally expected to degrade during or after tissue formation. The ideal hydrogel should degrade completely when the new tissue is formed. To achieve this goal, many attempts have been made to impart biodegradability to the most frequently used poly(ethylene glycol) (PEG) hydrogel. For example, oligomers of polyesters such as polycaprolactone and polylactide modified with acrylates have been incorporated into PEG to obtain photo-cross-linkable macromers for further biodegradable hydrogel fabrication.[17−19] Recently, Elisseeff's and Leong's groups reported photopolymerized hydrogels for cell encapsulations, taking advantage of the effect of polyphosphoesters (PPEs) on the biocompatibility, biodegradability, and hydrophilicity of PEG.[20,21] The macromers were formed either by modification of PEG with phosphoesters to generate photo-cross-linkable chain ends, or by conjugating PEG molecules with photo-cross-linkable groups to side chains of PPE. The synthesis was processed either through multistep reactions or in a less controllable fashion, both of which would make it difficult to control the structure of the macromer and the properties of the resultant hydrogel.

In this contribution, we attempted to synthesize photopolymerized hydrogels based on copolymers of PEG and PPEs with adjustable properties for tissue engineering by a simple procedure. We developed a one-step method to synthesize the photo-cross-linkable macromers based on copolymers of PEG and PPE by direct ring-opening polymerization of a cyclic phosphoester monomer that contains a double bond under the initiation of PEG and catalysis of stannous octoate. The macromers were further photopolymerized to form hydrogels. Herein, the polymerization is conducted in a relatively controllable fashion. The phosphoester contents can be easily adjusted by changing the feed ratio of the monomer to the PEG macroinitiator. Therefore, macromers with designed compositions and hydrogels with expectant properties can be obtained. In addition, part of the double bonds in the side chains of the macromers could be potentially modified for specific applications, while reserving the ability to form hydrogels. The physical and chemical properties of hydrogels, in vitro cytotoxicity, and potential application as scaffolds in tissue engineering were studied.

* Corresponding author.
[†] Department of Polymer Science and Engineering, University of Science and Technology of China.
[‡] Hefei National Laboratory for Physical Sciences at Microscale and School of Life Sciences, University of Science and Technology of China.
[§] Chinese Academy of Sciences.

10.1021/bm700474b CCC: $37.00
Published on Web 09/29/2007

2. Experimental Section

2.1. Materials. 2-Chloro-2-oxo-1,3,2-dioxaphospholane (COP) was synthesized by a method described previously[22] and distilled under reduced pressure before use. 2-Hydroxyethyl methacrylate (HEMA, Acros Organics, 98%) was distilled under reduced pressure before use. Triethylamine (TEA) was refluxed with phthalic anhydride, then with potassium hydroxide, and distilled. PEG diol (M_n = 3400 g/mol, PEG3400, Acros Organics) was dried twice by azeodistillation of toluene. Stannous octoate ($Sn(Oct)_2$, Sinopharm Chemical Reagent Co., Ltd., China) was purified according to a method described in the literature.[23] Tetrahydrofuran (THF) was refluxed with calcium hydride, and distilled over a Na−K alloy prior to use. The cytocompatible UV photoinitiator Irgacure 2959 (I2959, 2-hydroxy-1-[4-(hydroxyethoxy) phenyl]-2-methyl-1-propanone) was obtained from Ciba-Geigy Chemical Co. (Tom River, NJ). Other solvents or chemicals were used as received.

2.2. Synthesis. *2.2.1. Monomer 2-(2-oxo-1,3,2-dioxaphospholoyloxy) ethyl methacrylate (OPEMA).* OPEMA was synthesized according to the literature.[24] Briefly, into a 250 mL flame-dried three-necked flask equipped with a dropping funnel and a stir bar were added HEMA (10.0 g, 0.077 mol), TEA (7.8 g, 0.077 mol), and 100 mL of fresh dried THF. After cooling for 30 min at −10 °C, 11.0 g (0.077mol) of COP in 40 mL of THF was added dropwise to the stirred solution over a period of 30 min. The mixture was maintained at −10 °C overnight. The precipitate in the mixture, which was triethylammonium chloride, was then filtered off using a Schlenk funnel. The filtrate was concentrated under reduced pressure, and 50 mL of fresh dried diethyl ether was added to precipitate the small amount of triethylammonium chloride. After removal of the solvent under vacuum, the product OPEMA was obtained (yield: 90%). ^{1}H NMR ($CDCl_3$, ppm), 1.95 (−C***H***$_3$, 3H), 4.10−4.50 (−C***H***$_2$−, 8H), 5.60 (−C***H***═, 1H), 6.19 (−C***H***═, 1H).

2.2.2. Macromer POPEMA−PEG−POPEMA. The macromers were synthesized in a glove box with a water content of less than 0.1 ppm. In a typical procedure, PEG3400 (1.00 g), OPEMA (1.67 g), and 7 mL of THF were consecutively added into the reaction flask. After stirring at 50 °C for 30 min, stannous octoate (0.30 mmol) was added quickly. The reaction was carried out at 50 °C for an additional 24 h. The mixture was concentrated under reduced pressure and precipitated into cold ether to obtain the macromer.

2.2.3. Hydrogel. A 150 μL portion of the macromer solution (23%, w/v in double-deionized water) with 0.05 wt % I2959 was pipetted into the tissue culture inserts with a diameter of 8 mm, and exposed to long wavelength ultraviolet light (365 nm), provided by a UV light supplier (EXFO Omnicure 1000, Canada). The photopolymerization reaction was allowed to proceed for 5 min at a light density of 3−5 mW/cm^2 to form the hydrogel.

2.3. Characterization. *2.3.1. General Characterization.* ^{1}H NMR spectra were recorded on a Brucker AV300 NMR spectrometer at room temperature with $CDCl_3$ as the solvent and TMS as the internal reference. Fourier transform infrared (FT-IR) spectra were measured on a Bruker Vector 22 Fourier transform infrared spectrometer using the KBr disk method. Molecular weights and molecular weight distributions were determined by gel permeation chromatography (GPC) measurements. The GPC system is composed of a Waters 1515 pump and a Waters 2414 refractive index detector equipped with Waters Styragel high-resolution columns (HR4, HR2, HR1, and HR0.5; effective molecular-weight range: 5000−500 000, 500−20 000, 100−5000, and 0−1000, respectively) at 40 °C. Chloroform (HPLC grade, J. T. Baker, stabilized with 0.75% ethanol) was used as the mobile phase, delivered at a flow rate of 1.0 mL min^{-1}. Monodispersed polystyrene standards with a molecular weight range of 1310 to 5.51 × 10^4 were used to generate the calibration curve.

2.3.2. Swelling of Hydrogel. The hydrogel samples made as above were dried at 60 °C for 48 h and weighted as W_d. The swelling ratio determination was carried out in double-deionized water at 37 °C. At a predetermined time, the swollen samples were taken out and wiped slightly with filter paper to remove water on the surface, and weighted as W_t. The measurements continued until a constant weight was reached. The swelling ratio (q) was calculated by

$$q = \frac{W_t}{W_d} \times 100\%$$

All the experiments were carried out in triplicate, and the average values were reported.

2.3.3. Estimation of Network Parameters. The number-average molecular weight between cross-links, M_c, and the mesh size, ξ, was estimated according to the method by Canal and Peppas[25] using the equation listed below.

$$\frac{1}{M_c} = \frac{2}{M_n} - \frac{(\nu/V_1)[\ln(1-\nu_{2,s}) + \nu_{2,s} + \chi\nu_{2,s}^{\ 2}]}{\nu_{2,r}\left[\left(\frac{\nu_{2,s}}{\nu_{2,r}}\right)^{1/3} - \frac{1}{2}\left(\frac{\nu_{2,s}}{\nu_{2,r}}\right)\right]}$$

In this equation, M_n is the number-average molecular weight of the macromer determined by ^{1}H NMR, V_1 is the molar volume of water (18.035 cm^3/mol),[21] ν is the specific volume of the macromer (0.785 for PEG derivatives),[21] χ is the Flory polymer−solvent interaction parameter (for a PEG−water system, the value is 0.426),[26] and $\nu_{2,r}$ and $\nu_{2,s}$ are the polymer volume fractions before and after swelling, respectively, calculated according to the literature.[27] Here, the parameters of the PEG homopolymer were used without modification considering the limited content of PPE compared to the PEG segments. To calculate ξ, M_c was used to estimate the end-to-end distance of the unperturbed state $(\bar{r}_0^{\,2})^{1/2}$ along with the characteristic ratio, C_n, of the polymer chain according to

$$(\bar{r}_0^{\,2}) = l(2M_c/M_r)^{1/2}C_n^{\,1/2}$$

M_r is the molecular weight of the repeating units, the C−C bond length is given by l (1.54 Å), and the characteristic ratio C_n of the macromer was approximately 14, which is the C_n of PEG.[28] Accordingly, the mesh size ξ was obtained using the following equation:

$$\xi = \nu_{2,s}^{\ -1/3}(\bar{r}_0^{\,2})^{1/2}$$

2.3.4. Scanning Electron Microscopy (SEM). To visually examine the surface and interior structure of the hydrogel in swollen state, a JEOL model JSM-6700F SEM was used to analyze the pore structure. The hydrogel samples were swollen in water for 24 h to reach equilibrium, and then quickly put into liquid nitrogen for 10 min and transferred to a freeze-dryer for 72 h. The samples were then loaded on the surface of an aluminum SEM specimen holder and sputter coated with gold for 60 s before observation. An accelerating voltage of 10 kV was used to obtain the high-resolution images of the hydrogel samples. The magnification was varied from 500× to 5000× depending on the specific specimen.

2.3.5. Degradation of Hydrogel. The degradation experiment was conducted at different buffers at pH 4.0 (HOAc/NaOAc, 0.1 mol/L), 7.4 (phosphate buffer, 0.1 mol/L), or 10.0 ($NaHCO_3/Na_2CO_3$, 0.1 mol/L). Prior to the degradation experiments, triplicate samples were extracted with chloroform for 24 h at room temperature, then dried and weighted as W_d. Subsequently, the samples were immersed in buffers and incubated at 37 °C. At different time intervals, the samples were taken out, rinsed thoroughly with deionized water at 4 °C, lyophilized, and weighted as W_f. The percentage of weight loss was calculated as $\{W_d - W_f\}/W_d \times 100\%$.

2.4. Mouse Osteoblast Cell Isolation and Culture. Mouse osteoblasts were obtained from the long bones of young adult (4−6 weeks old) ICR mice. Following euthanasia by ethyl ether inhalation, femora were aseptically excised, cleaned of soft tissue, and washed in phosphate-buffered saline (PBS). The metaphyseal ends were cut off, and the marrow was flushed out from the midshaft with 5 mL of PBS

Scheme 1. Synthetic Routes of OPEMA Monomer and POPEMA−PEG−POPEMA Macromer

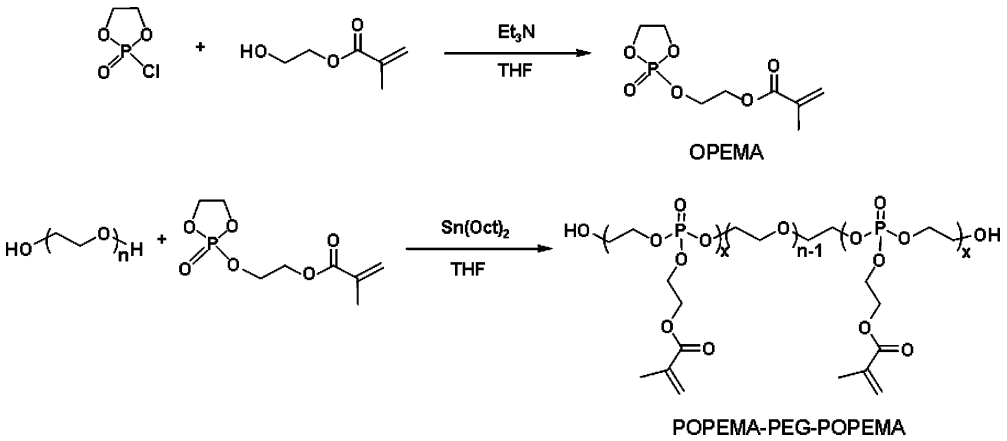

using a syringe equipped with a 27-gauge needle. The clean diaphyses were cut into small pieces of 1−2 mm using scissors. The bone pieces were then washed with PBS and incubated with collagenase II (2 mg/mL, Sigma) in Dulbecco's modified Eagle's medium (DMEM) at 37 °C in a shaking water bath to remove all soft tissue residual and adhering cells. After 2 h of incubation, 4 mL of DMEM supplemented with penicillin (100 U/mL), streptomycin sulfate (100 U/mL), gentamycin (50 μg/mL), fungizone (1.25 μg/mL, Sigma), ascorbate (100 μg/mL, Sigma), and 10% fetal bovine serum (Hyclone) was added to inhibit the activity of collagenase. The bone pieces were further rinsed three times, and transferred to 25-cm^2 culture flasks containing 5 mL of complete medium described above at a density of 20−30 fragments per flask. After 11−15 days of incubation at 37 °C in 5% CO_2, the osteoblasts were harvested and used in all the experiments.

2.5. 3-(4,5-Dimethylthiazol-2-yl)-2,5-diphenyltetrazolium Bromide (MTT) Assay. The cytotoxicity of macromers was evaluated in comparison with polyethylene glycol diacrylate (PEGDA, 3400 g/mol, Shearwater Polymers, Inc.). Osteoblast cells were seeded in a 96-well plate (Becton-Dickinson, Lincoln Park, NJ) with 100 μL of complete DMEM at a density of 6500 osteoblast cells per well. Cells were incubated for 24 h at 37 °C followed by replacing the culture medium with the solution of macromer or PEGDA (100 μL in complete DMEM) to achieve various carrier concentrations ranging from 0 to 1 mg/mL. Following 96 h of incubation, 25 μL of MTT solution (5 mg/mL in PBS) was added, and the plates were incubated at 37 °C for an additional 2 h. To each well was added 100 μL of the extraction buffer (20% sodium dodecyl sulfate (SDS) in 50% dimethylformamide), and the plate was incubated overnight at 37 °C. The optical density at 570 nm in each well was measured on a microplate reader (model 680, Bio-Rad Laboratories, Hercules, CA) using wells without MTT addition as the blank.

2.6. "Live/Dead" Assay. Osteoblasts were suspended in each macromer solution (23% w/v) containing 0.05% I2959 at a density of 10×10^6 cells/mL, and the macromer was photopolymerized under the same conditions described above. The cell/polymer constructs were cultured on an orbital shaker (50 rpm) in an incubator (5% CO_2, 37 °C). One day later, the initial viability of the encapsulated cells was determined using a LIVE/DEAD Viability/Cytotoxicity Kit (Molecular Probes, L-3224) according to the protocol provided by the supplier. The constructs were rinsed by PBS twice and incubated in PBS containing calcein-AM (2 μM) and ethidium homodimer-1 (4 μM) at 37 °C in 5% CO_2 for 10 min. Live and dead cells were imaged using a Zeiss LSM510 confocal laser scanning microscope.

3. Results and Discussion

We recently studied the kinetics and mechanism of cyclic phosphoester monomer polymerization under the co-initiation of stannous octoate and an alcohol. It has been demonstrated that the cyclic monomer, namely, 2-ethoxy-2-oxo-1,3,2-dioxaphospholane (EEP), can be polymerized with dodecanol/$Sn(Oct)_2$ with the living polymerization characteristic under mild conditions.[29] Stannous octoate ($Sn(Oct)_2$) is one of the most frequently used catalysts for ring-opening polymerization of lactone and lactide because of its high catalytic activity, as well as its U.S. FDA approval as a food additive.[30,31] In this study, we first synthesized the monomer OPEMA containing a photopolymerizable double bond (C═C) according to the literature[24] as shown in Scheme 1. The macromers were further synthesized using PEG3400 to initiate OPEMA polymerization with $Sn(Oct)_2$ as the catalyst.

Table 1. Composition and Molecular Weights of POPEMA−PEG−POPEMA Macromers

samples	OPEMA/PEG[a]	POPEMA−PEG−POPEMA[b]	M_n (g/mol)[c]	PDI[d]
macromer-1	8.5/1.0	$POPEMA_{1.5}$−PEG−$POPEMA_{1.5}$	4110	1.18
macromer-2	14.4/1.0	$POPEMA_{2.8}$−PEG−$POPEMA_{2.8}$	4720	1.20
macromer-3	24.0/1.0	$POPEMA_{4.3}$−PEG−$POPEMA_{4.3}$	5430	1.25

[a] Molar feed ratio of OPEMA to PEG. [b] The number subscript denotes the degree of polymerization of POPEMA on average, determined by ^{1}H NMR. [c] Determined by ^{1}H NMR. [d] Determined by GPC.

Detailed information of the macromers is summarized in Table 1. As one can see, upon increasing the feeding ratio of OPEMA to PEG3400, the phosphoester contents in the macromer increased gradually. The monomer conversions varied in the range of 35−39%, which was lower than that of EEP.[29] This might be due to the possible impurities of monomer, considering OPEMA cannot be purified by distillation like EEP. However, we are still capable of controlling the polymer compositions using this synthesis method. GPC measurements revealed that the molecular weight distribution was narrow with a polydispersity index (PDI) of around 1.2.

The chemical structure of the macromer was verified by NMR analyses. Figure 1 presents the ^{1}H NMR spectra of the three macromers with different phosphoester contents. Peaks at 4.2−4.4 ppm were assigned to the methylene protons from the backbone (g) and side chains (e+f) of the phosphoester units, which were overlapped because of the similar chemical environment. Peaks at 3.65 ppm (d) were assigned to methylene protons of PEG segments (−C$\boldsymbol{H}_2$C$\boldsymbol{H}_2$O−). Signals at 6.18 (a) and 5.61 ppm (b) were due to the conjunctional methylidene protons of the double bond (C$\boldsymbol{H}_2$═), and the methyl protons (−C$\boldsymbol{H}_3$) of the phosphoester units gave a signal at 1.95 ppm. No signal from stannous octoate was detected in the final polymer by ^{1}H NMR measurement. The integral area ratio of a/b/c/g was approximately 1:1:3:4. The result was in good agreement with

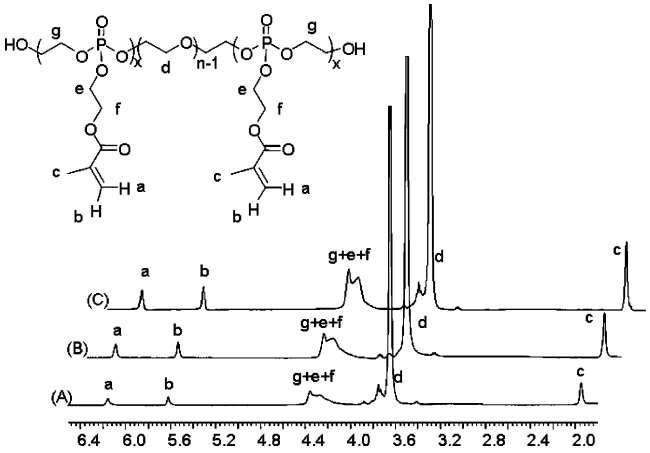

Figure 1. ^{1}H NMR spectra of (A) POPEMA$_{1.5}$−PEG−POEPEMA$_{1.5}$, (B) POPEMA$_{2.8}$−PEG−POEPEMA$_{2.8}$, and (C) POPEMA$_{4.3}$−PEG−POEPEMA$_{4.3}$ in $CDCl_3$.

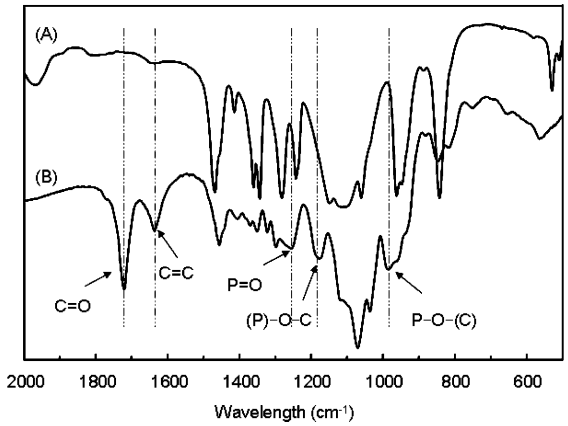

Figure 2. FT-IR spectra of (A) PEG and (B) POPEMA−PEG−POPEMA macromer.

the theoretical value, which particularly revealed the intact presence of double bonds during the ring-opening polymerization process. The number of double bonds and the polymerization degree of the PPE were calculated according to the integration ratios of peaks c and d, which were 3.0, 5.6, and 8.6 per polymer chain on average for macromers 1−3, respectively, as shown in Table 1.

Comparison of FT-IR spectra between PEG3400 and macromer-3 as an example is depicted in Figure 2. Absorption (bands) at 1254 and 1176 cm^{-1} marked in Figure 2B were due to the asymmetrical and symmetrical P═O stretchings, respectively. The P−O−C stretching was also verified at 986 cm^{-1} in the spectrum of macromer-3, while the strong and mediate absorptions at 1720 and 1635 cm^{-1} were the characteristic signals of C═O and C═C stretchings, respectively. The absence of these absorptions in the spectrum of PEG3400 also suggested the successful attachment of phosphoester units to PEG chains.

The hydrogel is fabricated by UV irradiation in the presence of Irgacure 2959 as the photoinitiator. Irgacure 2959 is one of most frequently used photoinitiators for the development of biocompatible photopolymerizing polymers for biomedical and tissue engineering applications. It caused minimal toxicity over a broad range of mammalian cell types and species.[32,33] In the present work, the intensity of the UV light was 3−5 mW/cm^2, which is not expected to induce cytotoxicity. Higher UV light densities have been utilized to fabricate hydrogels and did not cause damage to cells.[20,21] The hydrogels described in the paper were denoted as Gel-1, Gel-2, and Gel-3, deriving from

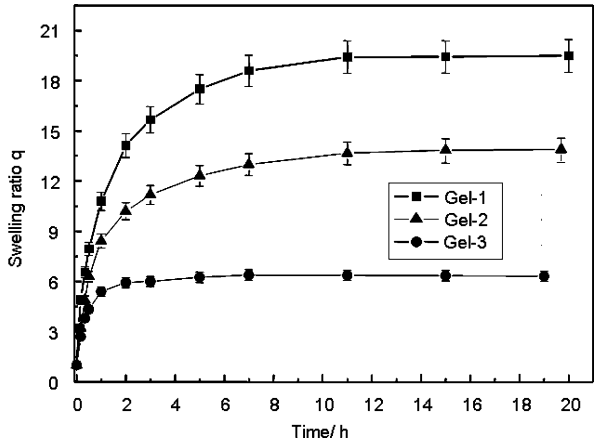

Figure 3. Swelling behavior of POPEMA−PEG−POPEMA hydrogels at 37 °C. The error bars represent the standard deviation ($n = 3$).

Table 2. Properties of Hydrogels Prepared from 23% (w/v) Macromer Solutions

samples	M_c (g/mol)	ξ (Å)
Gel-1	1528 ± 51	118.5 ± 4.4
Gel-2	1438 ± 93	110.8 ± 3.1
Gel-3	315 ± 5	38.3 ± 0.5

macromer-1, macromer-2, and macromer-3, respectively. The covalent cross-linking of double bonds is expected to produce a three-dimensional structure, which will swell but not disassociate in aqueous solution. The conversion of the macromers to the hydrogels was in the range of 70−83%, depending on the double-bond contents. The swelling behavior of these hydrogels, which impacts solute transport and cell viability from a tissue engineering perspective,[34] was measured and given in Figure 3.

As expected, a decrease in the swelling ratio is observed upon increasing the double bond content, which resulted in increased cross-linking density. For example, the swelling ratio of Gel-1 is 19.4 ± 0.3. It decreased to 13.8 ± 0.6 and 6.4 ± 0.2 for Gel-2 and Gel-3, respectively. The time for reaching swelling equilibrium also decreased with the increase of double-bond content, but all within 20 h. To estimate the hydrogel structure exhaustively, the number-average molecular weight between two cross-links (M_c) and the average mesh size (ξ) were calculated using the method proposed by Canal and Peppas.[25] As listed in Table 2, Gel-1 gave the highest M_c value (1528 g/mol) and the largest mesh size ξ (118.5 Å), exhibiting the lowest cross-linking density among the three hydrogels. In contrast, the cross-linking density of Gel-3 is the highest, giving an M_c of 315 g/mol and ξ at 38.3 Å. The difference is obviously attributed to the varied contents of the double bonds of the macromers. In other words, by controlling the macromer composition through adjusting the feeding ratio of OPEMA to PEG3400 during synthesis, the swelling ratio of hydrogel can be conveniently modulated to achieve the requirements for specific application in tissue engineering.

To examine the surface and interior structure of the hydrogel in the swollen state, SEM measurement was performed. SEM technique is useful to reveal hydrogel structure, although the pretreatment of dehydration and/or fixation procedures for SEM examination may affect the morphology of a hydrogel.[35] High water contents of the hydrogels will likely result in highly macroporous sponge-like scaffolds upon lyophilization. As shown in Figure 4, all of the hydrogel samples exhibited porous structures, while pore structures depended on the cross-linking

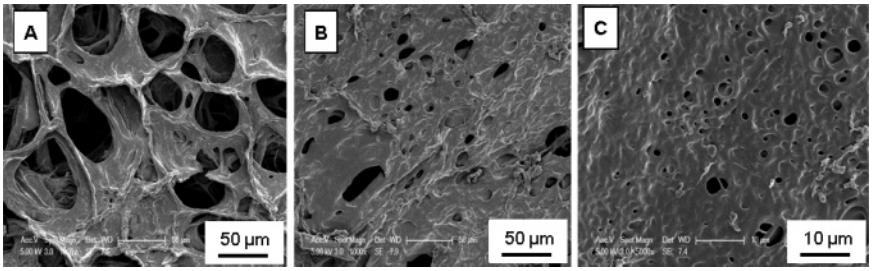

Figure 4. SEM micrographs of the hydrogels (A) Gel-1, (B) Gel-2, and (C) Gel-3 before degradation.

density of the hydrogels. The surface of Gel-1 shown in Figure 4A is rough and filled with interconnected circular or elliptical macropores. Porous structures were also observed in Figure 4B and 4C for Gel-2 and Gel-3, but their surfaces were less rough, and the pores were smaller. This trend of pore size variation is in agreement with the calculated values listed in Table 2. It was noticed that the visualized size of the lyophilized samples were larger than the calculated values in the swollen state. This may be due to the influence of the lyophilization process. Undoubtedly, well-controlled pore size is important in the design of the cellular matrix; however, identification of optimal conditions for a specific cell type remains to be a challenge because cell growth is believed to be affected by complex factors, although there have been a few reports describing the effects of pore size of the scaffold on cell growth.[36−38]

From the point of view of tissue engineering application, hydrogels with biodegradability are essentially needed since they will allow complete replacement by the regenerated tissue. Aliphatic polyesters have been widely used as biodegradable components of hydrogels because of the biocompatibility of the degradation products. In the present work, biodegradable and biocompatible PPE was introduced to fabricate the novel photo-cross-linked and biodegradable hydrogel. The versatility of the PPE structure may facilitate the adjustment of degradability by selecting a different backbone or side chains.[39] Degradation of hydrogel samples was carried out at three different pH values (pH 4.0, 7.4, and 10.0) in this study. Figure 5 shows the dependence of percent weight loss of hydrogels on degradation time under different pH conditions. It was found that the weight loss was strongly dependent on pH values. Gel-3 lost 48.8% of its weight at pH 10.0 after 106 days incubation, while only 27.9% and 18.8% weight lost was observed at pH 7.4 and 4.0 for the same period of incubation, respectively. The degradation trends of Gel-1 and Gel-2 were similar to that of Gel-3. This phenomenon is in agreement with that observed by Penczek's group.[40] They suggested that faster degradation of PPE in basic conditions was due to the simultaneous brokenness of phosphoester linkages in the main chain and the side chain, which would accelerate the disruption of the hydrogel networks in this study. While under acidic conditions, the degradation of PPE may occur mainly in the side groups, rendering the slow degradation of the hydrogel.

On the other hand, a comparison of hydrogel degradation at the same pH condition revealed that gels with higher cross-linking densities exhibited slow degradation properties. Gel-1 degraded completely in 25 days at pH 7.4, but Gel-3 only lost 27.9% of its weight, and Gel-2 was in the middle, with 79.9% weight loss after 106 days incubation under the same conditions. Similar trends were observed at pH 4.0 and 10.0. Gel-1 had the lowest cross-linking density among the hydrogels, bearing the loosest structure and the biggest pore sizes. It degraded completely in 3 days at pH 10.0. The fastest weight loss compared with that of the other two hydrogels was likely due

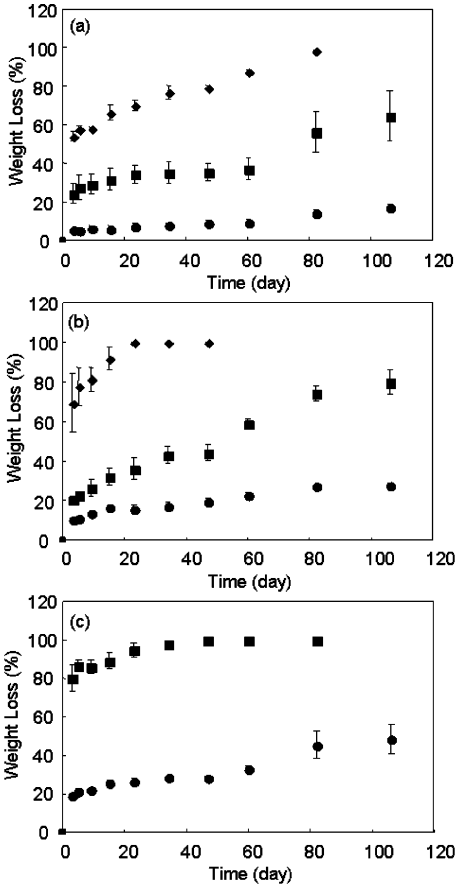

Figure 5. Degradation profiles of Gel-1 (diamond), Gel-2 (square), and Gel-3 (circle) at (a) pH 4.0 (HOAc/NaOAc), (b) pH 7.4 (PBS), and (c) pH 10.0 ($NaHCO_3/Na_2CO_3$), 37 °C. Mean ± standard deviation ($n = 3$).

to easier dissociation of the hydrogel network and diffusion of the degradation residue.

Degradation samples of the hydrogels were also characterized by SEM analysis. Figure 6 shows the SEM images of the surface and a cross-section of Gel-3 after degradation in PBS 7.4 at 37 °C. Before the degradation, only small cracks and pores were observed on the surface (Figure 4C), but after incubation at pH 7.4 for 106 days, the pores and cracks were distinct on the surface and also obvious inside the gel, which suggests that the hydrogel may degrade simultaneously in the bulk and on the surface, and the pores may be interconnected.

To investigate the potential of such gels in tissue engineering, cell cytotoxicity against osteoblasts in vitro was assessed for macromers by MTT assay, and the viability of cells encapsulated in the gel was also studied using live/dead assay. PEGDA and its photopolymerized hydrogel were used as the control since they have been extensively studied in tissue engineering. As shown in Figure 7, all three of the macromers did not exhibit significant cytotoxicity in cultured osteoblast cells with a

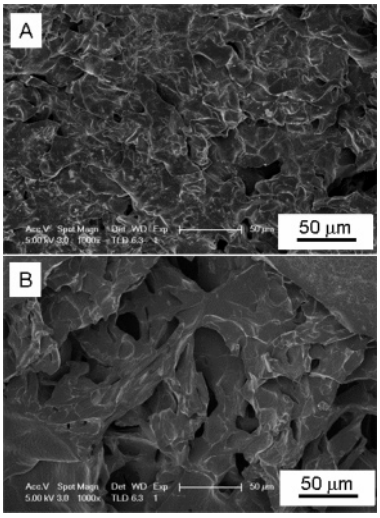

Figure 6. SEM micrographs of degraded Gel-3 after incubation in PBS at pH 7.4 and 37 °C for 106 days: (A) the surface region; (B) the cross-section.

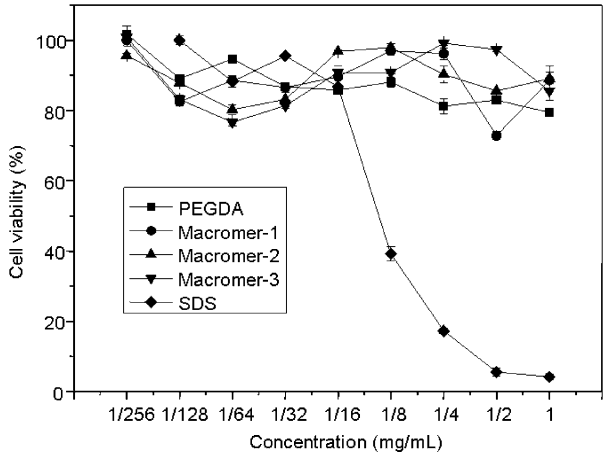

Figure 7. Cytotoxicity of macromers and PEGDA in comparison with SDS after 4 days of incubation with osteoblast cells. Mean ± standard deviation ($n = 3$).

concentration up to 1 mg/mL. In the live/dead assay for evaluation of cell viability, live cells are distinguished by their intracellular esterase activity, which is determined by the enzymatic conversion of nonfluorescent cell-permeable Calcein AM to an intensely green fluorescent calcein, while ethidium homodimer-1 enters cells with damaged membranes and attaches to nucleic acids within dead cells to produce red fluorescence.[41] Figure 8 shows the live/dead cell staining for different hydrogels. It was observed that the majority of osteoblast cells remained viable after 24 h of incubation in the hydrogels based on PPE and PEG copolymers. More cells encapsulated in these hydrogels remained viable than those in PEGDA-based hydrogel, which was in agreement with the MTT assay of the macromers.

In summary, we prepared novel biodegradable hydrogels based on PPE and PEG by UV photo-cross-linking. These hydrogels exhibited tunable properties, including swelling ratio, network parameters, and degradation rates. The syntheses of POPEMA−PEG−POPEMA macromers were by one-step ring-opening polymerization of OPEMA using PEG3400 as the initiator and $Sn(Oct)_2$ as the catalyst in a controllable fashion. PPE contents in macromers can be adjusted by tuning the ratio of OPEMA to PEG3400. The swelling ratio and network parameters changed regularly with the PPE content, while the degradability of the hydrogels was highly related to the cross-linking density and pH conditions. No significant cytotoxicity of the macromers against osteoblasts was observed up to 0.5 mg/mL, and most cells remained viable in these hydrogels, demonstrated by live/dead staining assay, suggesting potential application of these hydrogels in tissue engineering.

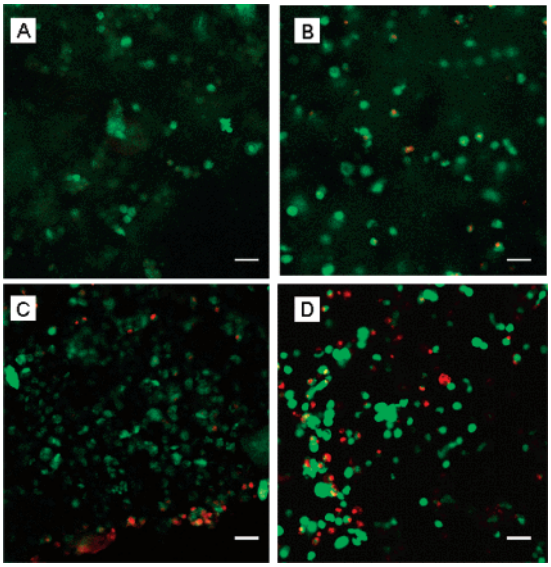

Figure 8. CLSM images of live (green) and dead (red) stained osteoblast cells encapsulated in (A) Gel-1,(B) Gel-2, (C) Gel-3, and (D) PEGDA hydrogel (bar = 40 μm).

Acknowledgment. We are thankful for the financial support from the National Science Foundation of China (20504025), the Ministry of Education of China (SRFDP Contract 20060358036), State Key Laboratory of Polymer Physics and Chemistry of Changchun Institute of Applied Chemistry, and the Bairen Program of the Chinese Academy of Sciences.

References and Notes

(1) Kissel, T.; Li, Y. X.; Unger, F. *Adv. Drug Delivery Rev.* **2002**, *54* (1), 99−134.
(2) Jeong, B.; Bae, Y. H.; Lee, D. S.; Kim, S. W. *Nature* **1997**, *388* (6645), 860−862.
(3) Horch, R. A.; Shahid, N.; Mistry, A. S.; Timmer, M. D.; Mikos, A. G.; Barron, A. R. *Biomacromolecules* **2004**, *5* (5), 1990−1998.
(4) Langer, R.; Peppas, N. A. *AIChE J.* **2003**, *49* (12), 2990−3006.
(5) Peppas, N. A.; Huang, Y.; Torres-Lugo, M.; Ward, J. H.; Zhang, J. *Annu. Rev. Biomed. Eng.* **2000**, *2*, 9−29.
(6) Peppas, N. A.; Hilt, J. Z.; Khademhosseini, A.; Langer, R. *Adv. Mater.* **2006**, *18* (11), 1345−1360.
(7) Park, Y.; Lutolf, M. P.; Hubbell, J. A.; Hunziker, E. B.; Wong, M. *Tissue Eng.* **2004**, *10* (3−4), 515−522.
(8) Nuttelman, C. R.; Henry, S. M.; Anseth, K. S. *Biomaterials* **2002**, *23* (17), 3617−3626.
(9) Mi, F. L.; Liang, H. F.; Wu, Y. C.; Lin, Y. S.; Yang, T. F.; Sung, H. W. *J. Biomater. Sci., Polym. Ed.* **2005**, *16* (11), 1333−1345.
(10) Tian, J.; Seery, T. A. P.; Weiss, R. A. *Macromolecules* **2004**, *37* (26), 9994−10000.
(11) Nguyen, K. T.; West, J. L. *Biomaterials* **2002**, *23* (22), 4307−4314.
(12) Hwang, N. S.; Varghese, S.; Theprungsirikul, P.; Canver, A.; Elisseeff, J. *Biomaterials* **2006**, *27* (36), 6015−6023.
(13) Drury, J. L.; Mooney, D. J. *Biomaterials* **2003**, *24* (24), 4337−4351.
(14) Nguyen, K. T.; West, J. L. *Biomaterials* **2002**, *23* (22), 4307−4314.
(15) Alhadlaq, A.; Elisseeff, J. H.; Hong, L.; Williams, C. G.; Caplan, A. I.; Sharma, B.; Kopher, R. A.; Tomkoria, S.; Lennon, D. P.; Lopez, A.; Mao, J. J. *Ann. Biomed. Eng.* **2004**, *32* (7), 911−923.
(16) Williams, C. G.; Kim, T. K.; Taboas, A.; Malik, A.; Manson, P.; Elisseeff, J. *Tissue Eng.* **2003**, *9* (4), 679−688.
(17) Behravesh, E.; Jo, S.; Zygourakis, K.; Mikos, A. G. *Biomacromolecules* **2002**, *3* (2), 374−381.
(18) Li, S. M.; Vert, M. *Macromolecules* **2003**, *36* (21), 8008−8014.
(19) Sawhney, A. S.; Pathak, C. P.; Hubbell, J. A. *Macromolecules* **1993**, *26* (4), 581−587.

(20) Li, Q.; Wang, J.; Shahani, S.; Sun, D. D. N.; Sharma, B.; Elisseeff, J. H.; Leong, K. W. *Biomaterials* **2006**, *27* (7), 1027−1034.
(21) Wang, D. A.; Williams, C. G.; Li, Q. A.; Sharma, B.; Elisseeff, J. H. *Biomaterials* **2003**, *24* (22), 3969−3980.
(22) Edmundson, R. S. *Chem. Ind.* **1962**, *1962*, 1828−1829.
(23) Kricheldorf, H. R.; Kreiser-Saunders, I.; Stricker, A. *Macromolecules* **2000**, *33* (3), 702−709.
(24) Ishihara, K.; Ueda, T.; Nakabayashi, N. *Polym. J.* **1990**, *22* (5), 355−360.
(25) Canal, T.; Peppas, N. A. *J. Biomed. Mater. Res.* **1989**, *23* (10), 1183−1193.
(26) Merrill, E. W.; Dennison, K. A.; Sung, C. *Biomaterials* **1993**, *14* (15), 1117−1126.
(27) Peppas, N. A.; Benner, R. E. *Biomaterials* **1980**, *1* (3), 158−162.
(28) Eichenbaum, K. D.; Thomas, A. A.; Eichenbaum, G. M.; Gibney, B. R.; Needham, D.; Kiser, P. F. *Macromolecules* **2005**, *38* (26), 10757−10762.
(29) Xiao, C. S.; Wang, Y. C.; Du, J. Z.; Chen, C. S.; Wang, J. *Macromolecules* **2006**, *39* (20), 6825−6831.
(30) Kricheldorf, H. R.; Kreiser-Saunders, I.; Stricker, A. *Macromolecules* **2000**, *33* (3), 702−709.
(31) Coulembier, O.; Degee, P.; Hedrick, J. L.; Dubois, P. *Prog. Polym. Sci.* **2006**, *31* (8), 723−747.
(32) Bryant, S. J.; Nuttelman, C. R.; Anseth, K. S. *J. Biomater. Sci., Polym. Ed.* **2000**, *11* (5), 439−457.
(33) Williams, C. G.; Malik, A. N.; Kim, T. K.; Manson, P. N.; Elisseeff, J. H. *Biomaterials* **2005**, *26* (11), 1211−1218.
(34) Lee, K. Y.; Mooney, D. J. *Chem. Rev.* **2001**, *101* (7), 1869−1879.
(35) Hong, P. D.; Chen, J. H. *Polymer* **1998**, *39* (23), 5809−5817.
(36) Dubruel, P.; Unger, R.; Vlierberghe, S. V.; Cnudde, V.; Jacobs, P. J.; Schacht, E.; Kirkpatrick, C. J. *Biomacromolecules* **2007**, *8* (2), 338−344.
(37) Vlierberghe, S. V.; Cnudde, V.; Dubruel, P.; Masschaele, B.; Cosijns, A.; Paepe, I. D.; Jacobs, P. J.; Hoorebeke, L. V.; Remon, J. P.; Schacht, E. *Biomacromolecules* **2007**, *8* (2), 331−337.
(38) Wachiralarpphaithoon, C.; Iwasaki, Y.; Akiyoshi, K. *Biomaterials* **2007**, *28* (6), 984−993.
(39) Zhao, Z.; Wang, J.; Mao, H. Q.; Leong, K. W. *Adv. Drug Delivery Rev.* **2003**, *55* (4), 483−499.
(40) Baran, J.; Penczek, S. *Macromolecules* **1995**, *28* (15), 5167−5176.
(41) Lin-Gibson, S.; Bencherif, S.; Cooper, J. A.; Wetzel, S. J.; Antonucci, J. M.; Vogel, B. M.; Horkay, F.; Washburn, N. R. *Biomacromolecules* **2004**, *5* (4), 1280−1287.

BM700474B